Study on Structure and Properties of SSBR/SiO_2 Co-coagulated Rubber and SSBR Filled with Nanosilica Composites

Xiao Liu,[1] Suhe Zhao[1,2]

[1]*Key Laboratory of Beijing City on Preparation and Processing of Novel Polymer Materials, Beijing 100029, China*
[2]*Key Laboratory for Nanomaterials, Ministry of Education, Beijing University of Chemical Technology, Beijing 100029, China*

Received 3 February 2008; accepted 30 April 2008
DOI 10.1002/app.28621
Published online 6 June 2008 in Wiley InterScience (www.interscience.wiley.com).

ABSTRACT: The morphological structure, glass transition, mechanical properties, and dynamic mechanical properties of star-shaped solution-polymerized styrene-butadiene rubber (SSBR) synthesized by a multifunctional organic lithium initiator and SiO_2-SSBR composite (N-SSBR) prepared through adding a small amount of nanosilica modified by silane coupling agent to star-shaped SSBR synthetic solution and co-coagulating, and their nanocomposites filled with 20 phr nanosilica were investigated, respectively. The results showed that the silica particles were well dispersed with nanosize in N-SSBR, which glass-transition temperature (T_g) was 2°C higher than SSBR. N-SSBR/SiO_2 nanocomposite exhibited lower Payne effect and internal friction loss, higher mechanical properties, and its T_g was 2°C higher than SSBR/SiO_2 nanocomposite. N-SSBR might promote the dispersion of nanosilica powder in matrix and could be applied to green tire tread materials. © 2008 Wiley Periodicals, Inc. J Appl Polym Sci 109: 3900–3907, 2008

Key words: dispersions; glass transition; morphology; nanocomposites; silicas

INTRODUCTION

Recently, the preparation of nanocomposite filled with inorganic nanoparticles has been of great interest for both academic researches and industrial applications. The key preparing technique of reinforced nanocomposite with good properties is the dispersion of nanoparticles in polymer matrix. Inorganic nanoparticles have the considerably large specific surface area and strong self-aggregation. Therefore, they should be modified by a silane coupling agent to be dispersed in polymer matrix with nanosize, and the organically modified nanoparticles may strongly interact with macromolecular chains. The desirable nanocomposite with good filler-dispersion is able to be prepared by a proper mixing.

Nowadays, there are mainly four methods for the preparation of nanocomposite filled with inorganic nanoparticles to have good dispersion: *in situ* polymerization dispersion, sol–gel, blending, and intercalation combination.[1–3] Among these approaches, the blending method is used widely for industrial applications.

The blending method includes melt compounding, solution compounding, and emulsion compounding. The melt compounding is that the nanoparticles are added to the melt matrix and mixed with matrix by a mechanical shearing. The solution compounding is that the organically modified particles are added to polymer solution. After the stirring to be dispersed homogeneously, the solvent has been removed, and the nanocomposite will be acquired. The emulsion compounding is that the nanoparticles are added to polymer emulsion, and after homogeneous stirring, demulsification, precipitating, cleaning, and drying, the nanocomposite will be prepared. In these methods, solution and emulsion compounding have been paid much attention at present.

Wang and coworkers[4–11] added the clay aqueous suspension to rubber latex, and then the rubber/clay nanocomposites had been obtained. Varghese et al.[12,13] added the layered silicate aqueous suspension into rubber latex to prepare the rubber/silicate nanocomposites. For the common hydrophilicity, nanofiller was dispersed in rubber latex easily, so the final nanocomposite exhibited excellent filler-dispersion in rubber matrix. However, there have been few studies on this solution compounding.

Both nanosilica and SSBR coupled by $SnCl_4$ have been the first choice for the preparation of green tire

Correspondence to: S. Zhao (zhaosh@mail.buct.edu.cn).
Contract grant sponsor: National Tenth-five Year Plan; contract grant number: 2004BA310A41.
Contract grant sponsor: National Natural Science Foundation of China; contract grant number: 50573005.

tread materials in rubber industry recently. Many researchers have made great efforts to resolve the problem of the combination of these two materials. The common method used to prepare nanocomposite is that the silica particles organically modified by a silane coupling agent are mixed with polymer in the mixing machines. Although the affinity between organically modified silica and rubber has been improved, the considerably large specific surface area and strong self-aggregation of organically modified silica particles are still not eliminated completely. Thus, with only mechanical mixing, it is hard to obtain SSBR/SiO_2 composite with nanosize filler-dispersion.

It is feasible to prepare the co-coagulated SiO_2-SSBR composite (N-SSBR) by adding a small quantity of organically modified nanosilica powder to the polymer solution, and stirring to be dispersed homogeneously, and then removing the solvent. In the processing, a large numbers of silica powder will be added to rubber matrix by a mechanical mixing. For the great affinity between silica powder in N-SSBR and silica powder subsequently added to rubber matrix, the subsequent silica powder will be mixed easily with N-SSBR and dispersed rapidly in matrix.

In this study, a little nanosilica powder was added to self-polymerized SSBR solution, and then the SiO_2-SSBR composite (N-SSBR) could be obtained by the co-coagulation. Three kinds of SSBR with different structural parameters were used to preparing co-coagulated rubbers in this manner. The mechanical properties, dynamic mechanical properties, and morphological structure of these co-coagulated rubbers as well as their nanocomposites filled with nanosilica had been studied, respectively. The significant conclusion could be drawn by comparing the structures and properties of N-SSBR/SiO_2 nanocomposites with those of SSBR/SiO_2 nanocomposites. It will provide the basic data for industrial production of SSBR/SiO_2 nanocomposites.

EXPERIMENTAL

Materials and compounding

The star-shaped SSBR with average four branches (the structural parameters of YK-1, YK-2, and YK-3 had been listed in Table I), which was synthesized by a homemade multifunctional organic lithium initiator, was produced by the Synthetic Rubber Plant of Yanshan Petrochemical Co. (Beijing, China). The precipitated silica (Tixosil 383) with an average particle diameter of 20–40 nm and specific surface area of 100–200 m^2/g came from Rhodia (Qingdao, China). The silane coupling agent was [3-(2-aminoethyl) aminopropyl] trimethoxy silane (AMMO) produced by Beijing Shenda Fine Chemical Co., (Beijing, China).

TABLE I
Structural Parameters of SSBR

Parameters	Compound no.		
	YK-1	YK-2	YK-3
Styrene content (%)	21.1	24.2	29.5
Vinyl content[a] (%)	38.1	46.0	34.7
M_n[b] ($\times 10^4$)	25.8	33.6	35.1
M_w[c] ($\times 10^4$)	39.2	61.3	57.4
Polydispersity index α[d]	1.52	1.82	1.63
Random degree[e] (%)	100	100	91.5

[a] The content of 1,2-butadiene structure.
[b] Number-average molecular weight.
[c] Weight-average molecular weight.
[d] The ratio of weight-average molecular weight to number-average molecular weight.
[e] The percentage of randomly distributed styrene monomer content in the total styrene content.

The other rubber additives, such as zinc oxide, stearic acid, and sulfur, were commercial grades.

Formulation

The formulation of SSBR/SiO_2 nanocomposites was as follows: 100 parts SSBR, 20 parts precipitated silica, 4 parts zinc oxide, 1 part stearic acid, 1.5 parts polymerized 2,2,4-trimethyl-1,2-dihydroquinoline, 1.2 parts benzothiazyl disulfide, 0.6 parts diphenyl guanidine, and 1.8 parts sulfur.

The overall content of the filler was 20 phr in each composite, and the mass fraction of AMMO was 7% of the mass of the nanosilica powder.

The samples are identified as follows:

YK-1, YK-2, and YK-3: Star-shaped solution-polymerized styrene-butadiene rubber (SSBR) with different structural parameters.

YK-1-0, YK-2-0, and YK-3-0: The co-coagulated rubbers containing a little nanosilica (N-SSBR); among these composites, YK-1-0 and YK-2-0 contained 3 phr nanosilica, and YK-3-0 contained 7 phr nanosilica.

YK-1-1, YK-2-1, and YK-3-1: SSBR/SiO_2 nanocomposites, which have 20 phr nanosilica.

YK-1-2, YK-2-2, and YK-3-2: N-SSBR/SiO_2 nanocomposites; the overall content of nanosilica in matrix remains 20 phr.

Preparation of N-SSBR

Preparation of organic silica powder

The nanosilica powder was added to the solution of ethanol-silane coupling agent, and then stirred homogeneously and settled for several hours. After the ethanol had vaporized entirely, the silica powder coated by a silane coupling agent was placed in an air oven at 80°C for 1 h to be ready to use in the next stage.

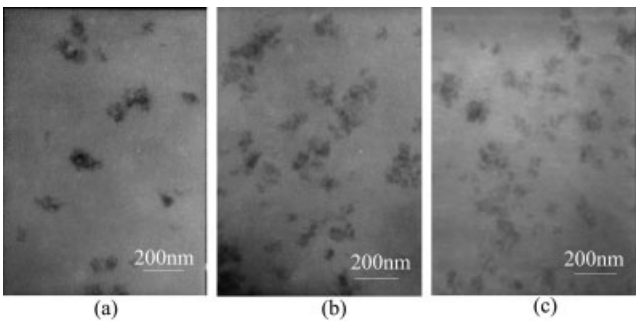

Figure 1 TEM photographs of co-coagulated rubbers: (a) YK-1-0, (b) YK-2-0, and (c) YK-3-0.

Preparation of N-SSBR

The organically modified silica powder was mixed with cyclohexane and stirred homogeneously, and then this solution mixture was added to SSBR solution and stirred homogeneously again. The SiO_2-SSBR composite (N-SSBR) could be obtained after the solvent had vaporized entirely.

Preparation of the vulcanizates

The rubber compounds were prepared with a 6-inch mill (Guangdong Zhanjiang Machinery Plant, Zhanjiang, China) with the conventional mixing technique. A plate vulcanization machine (Shanghai Rubber Machinery Works, Shanghai, China) was used to prepare the vulcanizates, and the curing condition was 150°C × t_{90} (curing time).

Instruments and techniques

Transmission electron microscopy (TEM) photographs of the microstructures of organically modified silica-SSBR composites were performed on an H-800-1 transmission electron microscope (Hitachi Corp., Tokyo, Japan), with an acceleration voltage of 200 kV.

The mechanical properties of all vulcanizates were measured at (25 ± 2)°C according to ASTM D638 with a CMT4104 electrical tensile tester (SANS, Shenzhen, China) at a tensile rate of 500 mm/min. The Shore A hardness of the vulcanizates was measured with a rubber hardness apparatus made by the 4th Chemical Industry Machine Factory (Shanghai, China).

Strain-sweep experiments were performed with an RPA 2000 rubber process analyzer (Alpha Technologies Co., Akron, Ohio, United States) at the frequency of 1 Hz and at 60°C for the vulcanizates. The strain was varied from 0.28 to 100%.

G' and tan δ as a function of the temperature were measured by a Dynamic Mechanical Thermal Analyzer DMTA V (Rheometrics Scientific, Piscataway, New Jersey, United States) at rectangular tension mode, 1 Hz and 3°C/min, and the strain amplitude was 0.005%. The temperature range was −100 to 100°C, and the samples were 2 mm in thickness and 6 mm in width.

RESULTS AND DISCUSSION

Morphological structure and glass transition of co-coagulated rubbers

Dispersion of nanosilica in N-SSBR

TEM photographs of YK-1-0, YK-2-0, and YK-3-0 are shown in Figure 1.

As shown clearly in Figure 1, the silica particles are dispersed in each sample with nanosize. It shows that the organically modified silica powder is able to be dispersed in the polymer solution by stirring. During the process of removing solvent, the macromolecular chains of rubber are gradually to get together and simultaneously wrap these nanoparticles to form the substantial nanoreinforced composites, which can be as new kind of matrix to be filled with other silica particles.

To carry out a quantitative analysis for the dispersion of silica in matrix, TEM images shown in Figure 1 were converted into the digital binary images shown in Figure 2 by the computer.[14] The details are as follows: first of all, highly contrasted pictures were obtained from the observed TEM images. Then, the digital binary images were prepared from the pictures through the image conversion. In the TEM photographs, silica particles in rubber matrix looked like a gray to dark colored phases, which were converted into black colored area in the digital binary images. Therefore, the rest of the picture, which showed white colored portion, corresponded to the rubber matrix. It can be seen that there are more silica particles in YK-3-0 because the silica content in YK-3-0 is more than that in YK-1-0 and YK-2-0. The area fraction of black colored portion (silica phase) of the picture (F_B) is shown at the bottom of

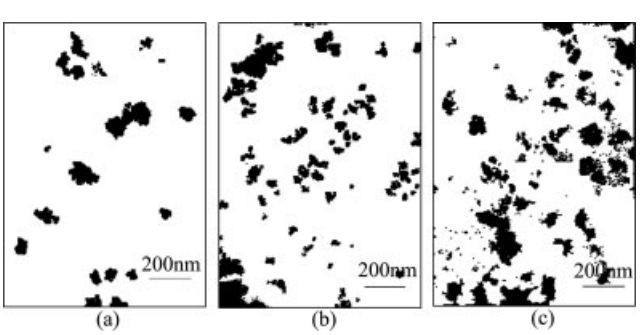

Figure 2 TEM digital binary photographs of co-coagulated rubbers: (a) YK-1-0 (F_B = 0.06 ± 0.01), (b) YK-2-0 (F_B = 0.09 ± 0.02), and (c) YK-3-0 (F_B = 0.16 ± 0.01).

images. From these data, YK-3-0 has remarkably higher F_B values than YK-1-0 and YK-2-0 in agreement with those observed TEM images. In this study, the digital binary images converted from TEM images show the two-dimensional information. However, TEM images actually involve the three-dimensional information due to the sample thickness. Thus it is possible that the observed F_B value is different from the factual one. From Figure 2, the dispersion of silica particles in YK-2-0 seems better than that in YK-1-0, thus it shows that the silica particles are dispersed easily in SSBR with high molecular weight.

Glass transition of composites

DMTA curves of YK-1 and YK-1-0, YK-2 and YK-2-0, and YK-3 and YK-3-0 are shown in Figure 3.

It is obviously seen in Figure 3 that G' values of two rubbers (YK-1 and YK-2) are nearly same as their corresponding co-coagulated rubbers (YK-1-0 and YK-2-0) in the region of glassy state. In the region of high-elastic state, YK-1 and YK-1-0 nearly exhibit the same G' values, as well as YK-2 and YK-2-0 exhibit a slight increment of 10–15% on G' values. This is mainly because the content of silica in N-SSBR is minor and double-strain amplitude brought on the rubber sample by the DMTA instrument is very low. It leads to a tiny stretching deformation, which does not exhibit the feature of composite reinforced by nanoparticles. For the composite (YK-3-0) which contains 7% silica, its G' value is larger than that of YK-3 with an increment of 22–26% in the region of glassy state, and with an increment of 21–32% in the region of high-elastic state.

In the region of glass-transition, G' values of three kinds of the co-coagulated rubbers (YK-1-0, YK-2-0, and YK-3-0) are larger than those of their corresponding pure rubbers (YK-1, YK-2, and YK-3) with the increment of 20–120%, 25–170%, and 0.3–21%, respectively. This result presents that the macromolecular chains of N-SSBR defreeze difficultly and are restrained as a result of the strong adsorption between organically modified nanosilica particles and macromolecular chains of rubber.

In Figure 3, the glass-transition temperatures of three pure rubbers (YK-1, YK-2, and YK-3) are different from one another, because they have different styrene content and vinyl content. The glass-transition temperature of YK-1 with lowest styrene content is the lowest, thus the styrene content is an important influencing factor of glass-transition temperature. The glass-transition temperatures of all the co-coagulated rubbers are 1 ~ 2°C higher than those of corresponding pure rubbers. The stronger adsorption between the organically modified nanosilica particles and macromolecular chains results in the lower flexibility of the macromolecular chains and higher glass-transition temperature of rubber.

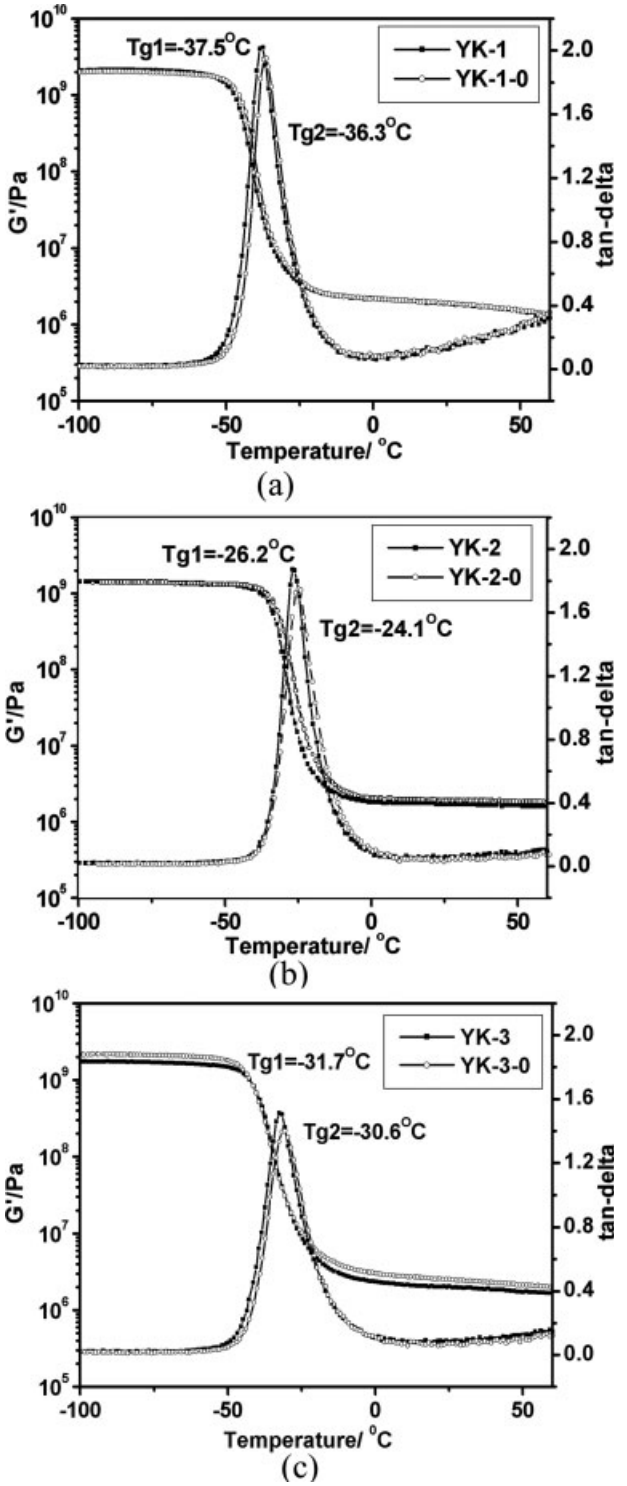

Figure 3 $G' \sim$ T and tan δ ~ T curves of crude rubbers and co-coagulated rubbers: (a) YK-1/YK-1-0, (b) YK-2/YK-2-0, and (c) YK-3/YK-3-0.

Compared with the corresponding pure rubbers, the values of tan δ peak height of the co-coagulated

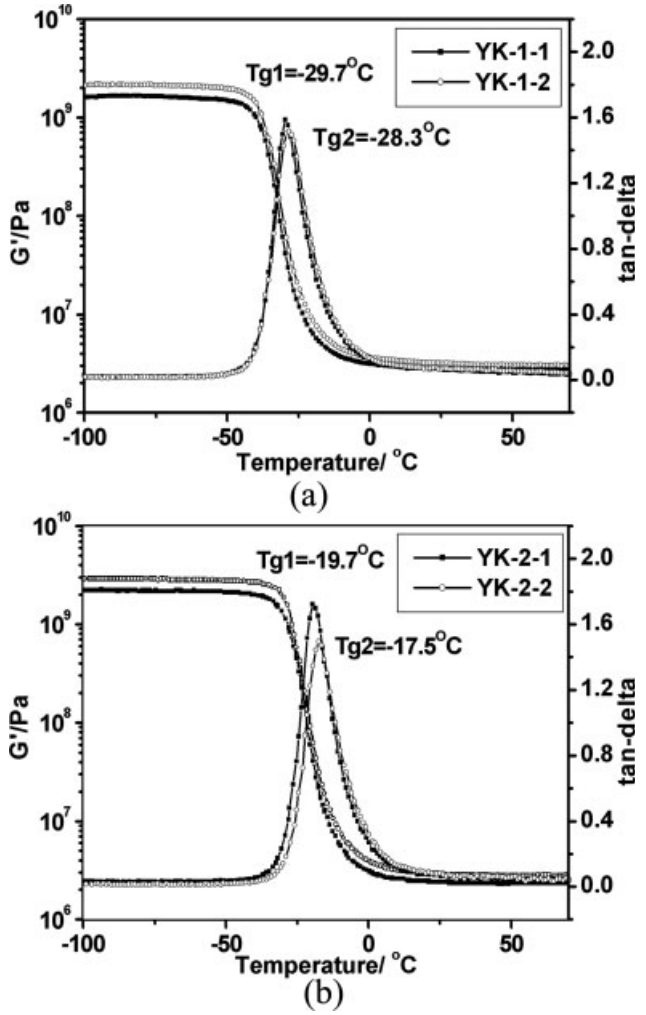

Figure 4 $G' \sim T$ and tan $\delta \sim T$ curves of SSBR/SiO_2 and N-SSBR/SiO_2 nanocomposites: (a) YK-1-1/YK-1-2 and (b) YK-2-1/YK-2-2.

rubbers in the region of glass-transition all drop and the values of peak area reduce. This indicates that during the defreezing process the internal friction loss of macromolecular chains reduces because of the adsorption between nanoparticles and partial macromolecular chains of rubber.

Structure and properties of SSBR/SiO_2 and N-SSBR/SiO_2 nanocomposites

Glass transition of nanocomposites

G' versus T and tan δ versus T curves of four vulcanizates (YK-1-1, YK-1-2, YK-2-1, and YK-2-2) are shown in Figure 4.

From Figure 4 it is clearly seen that, compared with SSBR filled with 20 phr organically modified silica, N-SSBR filled with the same amount of silica exhibit slightly higher G' values in glassy state, higher glass-transition temperatures, and lower values of internal friction loss in the region of glass-transition. These characteristics indicate that the nanosilica particles are dispersed in N-SSBR homogenously, and strongly interact with macromolecular chains of rubber. Moreover, the interfaces of silica particles can restrain the microvibration of macromolecular chains, and silica particles are dispersed in co-coagulated rubber with nanosize can promote the better dispersion of silica particles subsequently added to the co-coagulated rubber.

This result is the same as the other researchers' conclusion[15]: the more finely filler is dispersed in rubber matrix, the stronger interaction between filler and rubber exhibits. Besides the elastic modulus of composite increases and the loss modulus of composite decreases, the peak height and the peak area of tan δ reduce.

Figure 4 also presents that tan δ values of N-SSBR/SiO_2 nanocomposites are higher to some extent than those of corresponding SSBR/SiO_2 nanocomposites at 0°C, thus the N-SSBR/SiO_2 nanocomposites exhibit the better performance of wet-skid resistance.

From Figure 4, it can be seen that the glass-transition temperature and tan δ values at 0°C (i.e., wet-skid resistance) of YK-2-1 and YK-2-2 are higher than those of corresponding YK-1-1 and YK-1-2, respectively. It is possibly because YK-2 has higher vinyl content than YK-1 so the macromolecular chains are hard to relax.

Mechanical properties of nanocomposites

The mechanical properties of SSBR filled with 20 phr organically modified silica and N-SSBR filled with the same amount of silica are listed in Table II.

The data in Table II show that the scorch time and the optimum curing time of SSBR/SiO_2 nanocomposites are similar to those of N-SSBR/SiO_2 nanocomposites.

The tensile strength, tear strength, and modulus at 300% of N-SSBR/SiO_2 nanocomposites are slightly higher than those of SSBR/SiO_2 nanocomposites. It indicates that owing to mix silica with SSBR in two stages, the dispersion degree of nanosilica particles in N-SSBR/SiO_2 nanocomposites has been improved to some extent. Accordingly, the mechanical properties of N-SSBR/SiO_2 nanocomposites are slightly enhanced for the stronger interaction between filler and rubber as well as possibly better dispersion of silica in matrix.

The data in Table II shows that, YK-2-1 and YK-2-2 have relatively higher tear strength than other two series of samples. It is possibly because higher vinyl content of YK-2 leads to increasing chain tear resistance so that YK-2-1 and YK-2-2 samples need more strength to be torn.

TABLE II
Mechanical Properties of SSBR/SiO_2 and N-SSBR/SiO_2 Nanocomposites

Compound no.	YK1-1	YK1-2	YK2-1	YK2-2	YK3-1	YK3-2
t_{10}[a] (min)	3′10″	2′55″	2′49″	2′35″	1′51″	1′50″
t_{90}[b] (min)	16′35″	17′03″	19′14″	24′54″	19′47″	16′19″
Shore A hardness	56	56	57	57	56	56
Modulus at 300%[c] (MPa)	3.5	3.7	3.9	4.6	3.1	3.7
Tensile strength[d] (MPa)	9.8	10.7	10.3	11.9	8.9	10.3
Elongation at break[e] (%)	535	522	538	489	472	455
Permanent set[f] (%)	6	4	6	4	6	6
Tear strength[g] (KNm^{-1})	20.3	21.5	23.7	25.5	20.1	22.2

[a] Scorch time.
[b] Optimum curing time.
[c] The tensile stress necessary to elongate a specimen to 300% of its original length.
[d] The stress required to pull the specimen to the point where it breaks.
[e] The increase in length produced by stretching a test specimen to the breaking point expressed as a percentage of the initial length.
[f] The deformation remaining measured as elongation 3 min after the specimen was broken and reunited.
[g] The stress required to rip the specimen.

It can be seen from Table II that YK-3-1 and YK-3-2 have slightly lower elongation at break than other two series of samples. It is possibly because higher styrene content of YK-3 leads to difficult deformation and orientation of its macromolecular chains under tensile stress so that YK-3-1 and YK-3-2 samples are ruptured at lower elongation.

Dynamic mechanical properties of nanocomposites

G' versus ε% and tan δ versus ε% curves of all the vulcanizates are shown in Figures 5 and 6.

Figure 5 shows that, compared with SSBR/SiO_2 nanocomposites, the $\Delta G'$ (the difference value between G' in 0.28 and 100% of the strain) of N-SSBR/SiO_2 nanocomposites are lower (i.e., a lower Payne effect).[16] Payne effect usually is the measurement of the three-dimensional network construction for the filler-filler interaction and polymer-filler interaction. The lower Payne effect manifests the stronger polymer-filler interaction, better filler-dispersion, and lower internal friction loss between filler and polymer.

In Figure 6, during the zone of strain less than 10%, all the values of tan δ rise slightly with increasing the ε%. It is because the slide part of macromolecular chains increases with elevating the strain. The viscous stress and heat build-up of rubber increase rapidly through the friction among macromolecular chains. In the range of strain between 10 and 30%, the values of tan δ all reduce slightly with increasing the ε% for the G'' value decreases and G' value remains constant. It is possible that filler network has been destructed and has instantaneously separated from part of macromolecular chains. After the strain exceeds 30%, the values of tan δ all rise again for the micro-agglomerates destruction of filler. Then the entrapped rubber occluded in micro-agglomerates has been released, and the enlarged ''effective volume'' of free molecular chain segment leads to the increase of internal friction loss. Com-

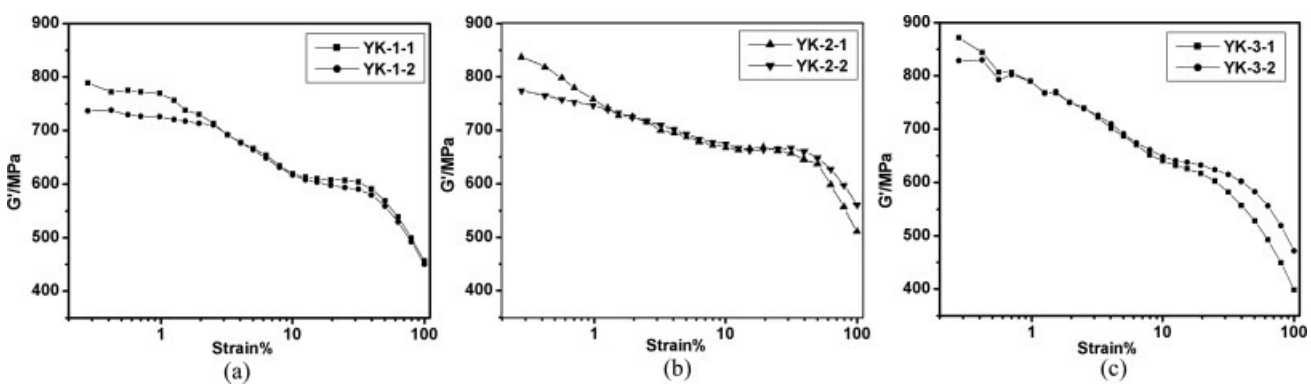

Figure 5 $G' \sim \varepsilon$% curves of SSBR/SiO_2 and N-SSBR/SiO_2 nanocomposites: (a) YK-1-1/YK-1-2, (b) YK-2-1/YK-2-2, and (c) YK-3-1/YK-3-2.

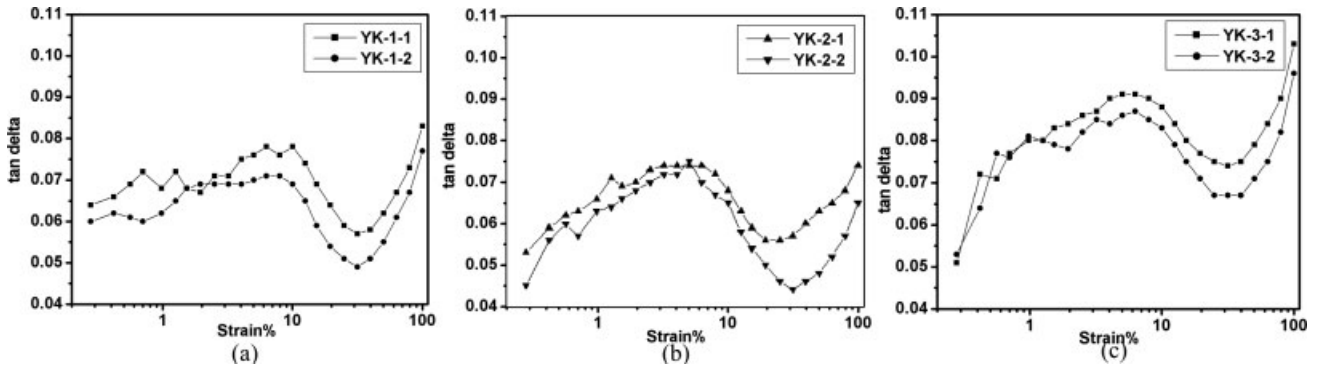

Figure 6 tan δ ~ ε% curves of SSBR/SiO_2 and N-SSBR/SiO_2 nanocomposites: (a) YK-1-1/YK-1-2, (b) YK-2-1/YK-2-2, and (c) YK-3-1/YK-3-2.

pared with SSBR/SiO_2 nanocomposites, the values of tan δ of N-SSBR/SiO_2 nanocomposites are all lower. These results manifest that the better filler-dispersion and stronger interfacial interaction are good for decreasing the interfacial slippage and internal friction among the interfaces of macromolecular chains, and therefore the value of internal friction loss of nanocomposite has reduced.

Figure 6 also shows that the tan δ values (i.e., internal friction loss values) of YK-3-1 and YK-3-2 are slightly higher than the other two series of samples. It is possibly because higher styrene content of YK-3 leads to severe friction among these rigid groups under a certain strain.

Morphological structure of nanocomposites

TEM photographs of the microstructure of the SSBR/SiO_2 and N-SSBR/SiO_2 nanocomposites are displayed in Figure 7.

From the photographs of N-SSBR/SiO_2 nanocomposites in Figure 7, it can be seen that silica particles are dispersed in SSBR matrix homogeneously as spherical shape. The dispersion of silica in N-SSBR is evidently superior to that in SSBR. N-SSBR with a small quantity of silica powder can help the subsequently added silica particles to be dispersed rapidly in matrix due to the common compatibility between silica particles in N-SSBR and silica particles added in the second step. Furthermore, the silica particles already dispersed in first step can hinder the aggregation of silica particles added in second step, thus the dispersion of the whole silica content is improved to some extent.

Figure 8 exhibits the digital binary images converted from TEM images shown in Figure 7. An indivisible flock of silica particles observed in the TEM images was defined as the agglomerate of filler particles. It can be clearly seen that the dimensions of silica agglomerates in SSBR/SiO_2 nanocomposites are all larger than those in N-SSBR/SiO_2 nanocomposites. The data of F_B are shown at the bottom of the images. Theoretically, all nanocomposites should have similar values of F_B since the silica content in all samples was set to be 20 phr. However, the values of F_B of SSBR/SiO_2 nanocomposites in which there are more agglomerates are higher than N-SSBR/SiO_2 nanocomposites. The different F_B values are possibly because of the difference between the TEM images which include three-dimensional information and the digital binary images which include two-dimensional information. Nevertheless, this difference of F_B values between SSBR/SiO_2 and N-SSBR/SiO_2 nanocomposites has exceeded the experimental error. Sawanobori et al.[17] reported that a certain amount of rubber molecules was entrapped in the agglomerates in silica filled rubber systems. According to this opinion, the aforementioned differ-

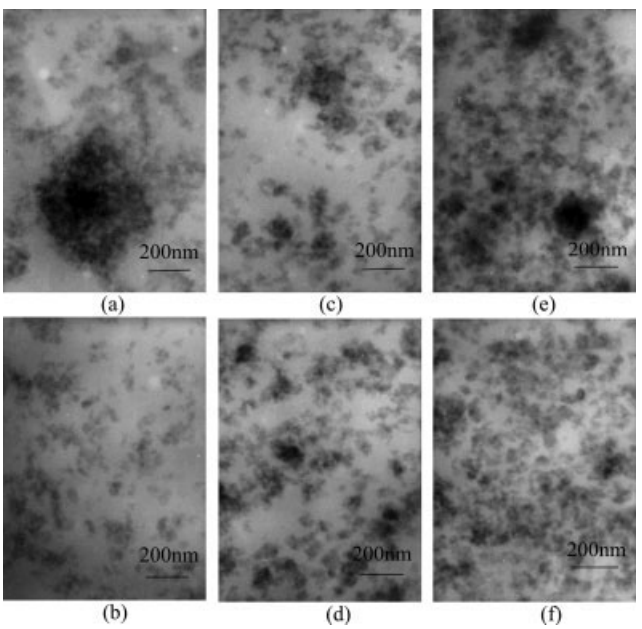

Figure 7 TEM photographs of SSBR/SiO_2 and N-SSBR/SiO_2 nanocomposites: (a) YK-1-1, (b) YK-1-2, (c) YK-2-1, (d) YK-2-2, (e) YK-3-1, and (f) YK-3-2.

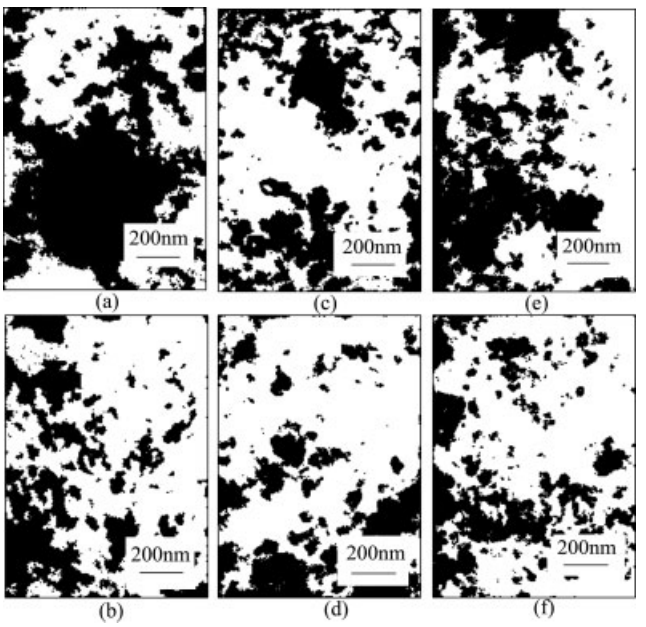

Figure 8 TEM digital binary photographs of SSBR/SiO_2 and N-SSBR/SiO_2 nanocomposites: (a) YK-1-1 (F_B = 0.56 ± 0.02), (b) YK-1-2 (F_B = 0.33 ± 0.01), (c) YK-2-1 (F_B = 0.38 ± 0.01), (d) YK-2-2 (F_B = 0.31 ± 0.01), (e) YK-3-1 (F_B = 0.45 ± 0.02), and (f) YK-3-2 (F_B = 0.30 ± 0.02).

ence can be explained. In N-SSBR/SiO_2 nanocomposites, the silica particles have been dispersed two times through adding them to matrix in two steps. Moreover, the silica particles in N-SSBR composite can promote the dispersion of silica subsequently added to matrix, thus it is easy to exhibit a smaller particle size and fewer agglomerates in N-SSBR/SiO_2 nanocomposites. On the contrary, SSBR/SiO_2 nanocomposites involve many agglomerates in which a certain amount of rubber is entrapped. During the conversion of observed TEM images into the digital binary images, the entrapped rubber occluded in agglomerates is converted into black colored area but the rubber matrix still exhibits white colored portion. With increasing the size of agglomerate, the amount of entrapped rubber increases, contributing to the increase in F_B value and difference of F_B values between SSBR/SiO_2 and N-SSBR/SiO_2 nanocomposites. Therefore, N-SSBR/SiO_2 nanocomposites with lower F_B values exhibit the relatively better filler-dispersion.

All the above results show that N-SSBR composites prepared by co-coagulation technique can improve the dispersion and homogeneity of nanosilica particles in matrix. In addition, the slight improvement of mechanical and dynamic mechanical properties of N-SSBR/SiO_2 nanocomposites also testifies that using co-coagulation technique for preparing the high-performance reinforced nanocomposite is an efficient way.

CONCLUSIONS

Adding organically modified silica powder to star-shaped SSBR solution directly, the co-coagulated SiO_2-SSBR composite (N-SSBR) has been obtained after the co-coagulation.

Either the glass-transition temperatures of SSBR or those of SSBR filled with 20 phr organically modified silica are 2°C lower than those of N-SSBR and N-SSBR filled with the same amount of silica, respectively. N-SSBR as well as N-SSBR/SiO_2 nanocomposites exhibit lower values of tan δ peak area. The better dispersion of nanosilica particles and stronger interfacial interaction can restrain the motion of the macromolecular chains.

In N-SSBR/SiO_2 nanocomposites, nanosilica particles with size range from 20 to 30 nm are dispersed in SSBR matrix homogeneously as the spherical shape.

The tensile strength, tear strength, and modulus at 300% of the N-SSBR/SiO_2 nanocomposites are all slightly higher than those of SSBR/SiO_2 nanocomposites. Moreover, the N-SSBR/SiO_2 nanocomposites have lower Payne effect and internal friction loss values.

References

1. Hsu, Y. G.; Chiang, I. L.; Lin, K. H. Mater Sci Eng B 2001, 87, 31.
2. Wang, C.; Wei, Y.; Ferment, G. R.; Li, W.; Li, T. Mater Lett 1999, 39, 206.
3. Kim, Y.; Lee, W. K.; Cho, W. J.; Ha, C. S.; Ree, M.; Chang, T. Polym Int 1997, 43, 129.
4. Wang, Y. Q.; Zhang, H. F.; Wu, Y. P.; Yang, J.; Zhang, L. Q. J Appl Polym Sci 2005, 96, 318.
5. Wang, Y. Q.; Zhang, H. F.; Wu, Y. P.; Yang, J.; Zhang, L. Q. Eur Polym J 2005, 41, 2776.
6. Wu, Y. P.; Wang, Y. Q.; Zhang, H. F.; Wang, Y. Z.; Yu, D. S.; Zhang, L. Q.; Yang, J. Compos Sci Technol 2005, 65, 1195.
7. Liang, Y. R.; Wang, Y. Q.; Wu, Y. P.; Lu, Y. L.; Zhang, H. F.; Zhang, L. Q. Polym Test 2005, 24, 12.
8. Wu, Y. P.; Jia, Q. X.; Yu, D. S.; Zhang, L. Q. J Appl Polym Sci 2003, 89, 3855.
9. Wu, Y. P.; Zhang, L. Q.; Wang, Y. Q.; Yu, D. S. J Appl Polym Sci 2001, 82, 2842.
10. Zhang, L. Q.; Wang, Y. Q.; Sui, Y.; Yu, D. S.; Wang, Y. Z. J Appl Polym Sci 2000, 78, 1873.
11. Wang, Y. Z.; Tang, C. H.; Yu, D. S.; Zhang, L. Q. J Appl Polym Sci 2000, 78, 1879.
12. Varghese, S.; Kocsis, J. K. Polymer 2003, 44, 4921.
13. Varghese, S.; Gatos, K. G.; Apostolov, A. A.; Kocsis, J. K. J Appl Polym Sci 2004, 92, 543.
14. Yatsuyanagi, F.; Suzuki, N.; Ito, M.; Kaidou, H. Polymer 2001, 42, 9523.
15. Wu, Y. P.; Zhang, L. Q.; Wang, Y. Z.; Wang, Y. Q.; Sun, Z. H.; Zhang, H. F.; Yu, D. S. Chin J Mater Res 2000, 14, 188.
16. Payne, A. R. J Appl Polym Sci 1962, 6, 57.
17. Sawanobori, J; Ono, S.; Ito, M. Jpn J Polym Sci Technol 2000, 57, 356.